JOURNAL OF EXTRACELLULAR VESICLES
2020, VOL. 9, 1766821
https://doi.org/10.1080/20013078.2020.1766821

Taylor & Francis
Taylor & Francis Group

RESEARCH ARTICLE

OPEN ACCESS Check for updates

Indoor dust extracellular vesicles promote cancer lung metastasis by inducing tumour necrosis factor-α

Nhung Thi Hong Dinh[a*], Jaewook Lee[a*], Jaemin Lee[a], Sang Soo Kim[a], Gyeongyun Go[a], Seoyoon Bae[a], Ye In Jun[a], Yae Jin Yoon[a], Tae-Young Roh[a,b] and Yong Song Gho[a]

[a]Department of Life Sciences, Pohang University of Science and Technology (POSTECH), Pohang, Republic of Korea; [b]Division of Integrative Biosciences and Biotechnology, Pohang University of Science and Technology (POSTECH), Pohang, Republic of Korea

ABSTRACT

Indoor pollutants are important problems to public health. Among indoor pollutants, indoor dust contains extracellular vesicles (EVs), which are associated with pulmonary inflammation. However, it has not been reported whether indoor dust EVs affect the cancer lung metastasis. In this study, we isolated indoor dust EVs and investigated their roles in cancer lung metastasis. Upon intranasal administration, indoor dust EVs enhanced mouse melanoma lung metastasis in a dose-dependent manner in mice. Pre-treatment or co-treatment of indoor dust EVs significantly promoted melanoma lung metastasis, whereas post-treatment of the EVs did not. In addition, the lung lysates from indoor dust EV-treated mice significantly increased tumour cell migration *in vitro*. We observed that tumour necrosis factor-α played important roles in indoor dust EV-mediated promotion of tumour cell migration *in vitro* and cancer lung metastasis *in vivo*. Furthermore, *Pseudomonas* EVs, the main components of indoor dust EVs, and indoor dust EVs showed comparable effects in promoting tumour cell migration *in vitro* and cancer lung metastasis *in vivo*. Taken together, our results suggest that indoor dust EVs, at least partly contributed by *Pseudomonas* EVs, are potential promoting agents of cancer lung metastasis.

ARTICLE HISTORY
Received 17 September 2019
Revised 4 May 2020
Accepted 4 May 2020

KEYWORDS
Extracellular vesicles; indoor dust; cancer lung metastasis; tumour cell migration; tumour necrosis factor-α

Introduction

According to US Environmental Protection Agency, indoor pollutants have been classified as one of the most important environmental problems to public health [1]. In modern life, people spend approximately 90% of their time for indoor activities [2], suggesting that indoor pollutants are strongly associated with public health. Persistent exposure to indoor pollutants is a potential threat to human health by causing respiratory diseases [3].

Among indoor pollutants, indoor dust contains various biological materials including extracellular vesicles (EVs) [4–6]. EVs are nano-sized, spherical and lipid-bilayered membranous structures that harbour different cargos such as lipids, proteins and nucleic acids [7,8]. These vesicles are universally secreted by all living cells and are found in various environments [9–13]. It has been shown that intranasal introduction of Gram-negative bacterial EVs in indoor dust could mediate neutrophilic pulmonary inflammation *in vivo* [5]. In addition, high levels of anti-dust EV IgG titres were detected in the patients with non-eosinophilic asthma, chronic obstructive pulmonary disease and lung cancer [14].

Tumour metastasis occurs when cancer cells from the primary sites spread to different sites or distant organs and is responsible for more than 90% of tumour-related deaths [15]. Metastasis to distant organs is strongly influenced by many factors like motility, invasion, plasticity, colonizing ability, angiogenesis and local microenvironments [16,17]. In addition, the lungs are directly exposed to indoor pollutants [18,19] and are one of the most common distant organs where tumour metastasis occurs [20]. However, to our best knowledge, there have been no evidences for the direct involvement of indoor pollutants in cancer lung metastasis.

In this study, we isolated and characterized indoor dust EVs. Then, we investigated whether indoor dust EVs, as a part of indoor pollutants, could affect cancer lung metastasis in a mouse metastatic melanoma model. To assess the underlying mechanism, we examined how tumour cells migrate upon treating indoor dust EVs or the lung lysates collected from indoor dust EV-treated mice. Finally, tumour necrosis factor-α

CONTACT Yong Song Gho ysgho@postech.ac.kr; Tae-Young Roh tyroh@postech.edu Department of Life Sciences, Pohang University of Science and Technology (POSTECH), POSTECH, 77 Cheongam-ro, Nam-gu, Pohang 37673, Republic of Korea
*These authors contributed equally to this work.

(TNF-α) knock-out mice were utilized to investigate the roles of TNF-α in enhancement of tumour cell migration *in vitro* and promotion of cancer lung metastasis *in vivo* mediated by indoor dust EVs.

Materials and methods

We have submitted all relevant data of our experiments to the EV-TRACK knowledgebase (EV-TRACK ID: EV200033) [21].

Mice

Animal experiments in this study were performed following the recommendations of the Institutional Animal Care and Use Committee at Pohang University of Science and Technology. The protocol was evaluated and approved by Institutional Animal Care and Use Committee at Pohang University of Science and Technology (Approval number: POSTECH-2016-0052-C1). Wild-type and TNF-α knock-out mice of the C57BL/6 background were obtained from Jackson Laboratories (Bar Harbor, ME, USA), and 4- to 5-week-old male mice were used for animal experiments. All mice used in this study were reared under specific pathogen-free conditions.

Cell culture

Mouse melanoma cells (B16BL6) and embryonic fibroblasts (NIH-3T3) were maintained in Minimum Essential Medium (MEM; Gibco, Carlsbad, CA, USA) and in Dulbecco's modified Eagle's medium (Gibco), respectively. All culture media included 10% foetal bovine serum (FBS), penicillin (100 units/mL) and streptomycin (0.1 mg/mL). All cells were cultured at 37°C with 5% CO_2 in a humidified incubator.

Isolation of indoor dust EVs and *Pseudomonas aeruginosa* EVs

Using a vacuum cleaner, indoor dust was harvested from the surfaces of floors, shelves and tables in randomly selected rooms throughout a dormitory building, as previously reported with some modifications [5]. Indoor dust was dissolved with phosphate-buffered saline (PBS) by stirring at 100 rpm for 12 h at 4°C. About 30 g of indoor dust was utilized for purifying indoor dust EVs. Twenty-five millilitres of PBS were utilized to dissolve 1 g of indoor dust, and there were no physical disruptions when dissolving indoor dust. Insoluble matters and cell debris were removed using gauze and centrifugation at 10,000 × *g* for 20 min at 4°C. The supernatant was filtrated with 0.45 and 0.22 μm pore-sized filters, then the filtrate was pelleted using ultracentrifugation at 150,000 × *g* for 3 h at 4°C, using Type 45Ti rotor (Beckman Coulter, Brea, CA, USA). To further purify indoor dust EVs, the pellet containing crude EVs was dissolved with 2.5 mL of 50% iodixanol (Sigma-Aldrich, St. Louis, MO, USA). The dissolved crude EVs were placed to the bottom of density gradients (1.25 mL of 10% iodixanol and 1.5 mL of 40% iodixanol). After buoyant density gradient ultracentrifugation at 200,000 × *g* for 2 h at 4°C using SW 55Ti rotor (Beckman Coulter), the fraction containing the purified indoor dust EVs was retrieved from the third fraction from the top, among 10 fractions with the same volume. Total protein concentration of the purified indoor dust EVs was quantified using Bradford assay (Bio-Rad Laboratories, Hercules, CA, USA). The indoor dust EVs were divided into several aliquots and stored at −80°C for further experiments.

P. aeruginosa EVs were isolated as previously reported [22] with some modifications. Briefly, *P. aeruginosa* PAO1 (American Type Culture Collection, Manassas, VA, USA) was cultured in lysogeny broth at 37°C with shaking at 150 rpm, until A_{600} = 1.5. Then, bacterial culture was centrifuged at 10,000 × *g* for 20 min at 4°C, and the supernatant was filtered using 0.45 μm pore-sized filters. The filtrate was concentrated with tangential flow filtration with 100 kDa hollow fibre membrane (GE Healthcare Bio-Sciences, Pittsburgh, PA, USA). The concentrate was filtered again with 0.22 μm pore-sized filters and subjected to ultracentrifugation at 150,000 × g for 3 h at 4°C, using Type 45Ti rotor. The pellet was resuspended in 50% iodixanol (final 2.4 mL) and applied to the bottom of iodixanol density gradient layers (1.0 mL of 10% and 1.5 mL of 40% iodixanol layers). After ultracentrifugation at 200,000 × *g* for 2 h at 4°C using SW 55Ti rotor, the fraction containing *P. aeruginosa* EVs was harvested from the third fraction from the top. The isolated EVs were aliquoted and stored at −80°C until use. Total protein concentration of *P. aeruginosa* EVs was determined using Bradford assay (Bio-Rad Laboratories).

Characterization of indoor dust EVs and *P. aeruginosa* EVs

Total particle concentration of indoor dust EVs was measured by nanoparticle tracking analysis with Nanosight LM10-HS system equipped with Nanoparticle Tracking Analysis software version 3.2 (Malvern Instruments Ltd., Malvern, UK), as previously reported [23]. Briefly, indoor dust EVs were diluted with PBS and subjected to measurement with the following settings: injection volume = 0.5 mL; laser wavelength = 405 nm; camera level = 12;

number of measurement = 3; measurement duration = 30 s; viscosity = 0.89 cP; chamber temperature = 25°C; detection threshold = 5; blur = auto; minimum track length = 10; minimum expected size = auto; range of detection = (0.8–2.5)×10^9 particles/mL.

The indoor dust EVs or *P. aeruginosa* EVs were placed on carbon-coated 400-mesh copper grids (Electron Microscopy Sciences, Matfield, PA, USA). After rinsing with deionized water, the EV-absorbed grids were subjected to negative staining with 1% uranyl acetate (Ted Pella, Redding, CA, USA). Transmission electron microscopy was conducted with JEM1011 microscope (JEOL, Tokyo, Japan), at an accelerating voltage of 100 kV.

The diameters of indoor dust EVs or *P. aeruginosa* EVs were determined using dynamic light scattering with Zetasizer Nano ZS equipped with Zetasizer Software version 6.34 (Malvern Instruments Ltd.). Indoor dust EVs or *P. aeruginosa* EVs were dispersed with PBS (1×10^9 particles/mL, final volume 1 mL) and subjected to analysis with the following parameters: laser wavelength = 633 nm; number of measurement = 5; measurement duration = 30 s; chamber temperature = 25°C.

To investigate the origin of indoor dust EVs, enzyme-linked immunosorbent assay (ELISA) was performed using various amounts of indoor dust EVs coated on 96 black well plates (Greiner Bio-One Ltd., Frickenhausen, Germany) for overnight. After blocking the plates with 3% bovine serum albumin in PBS for 1 h, anti-lipid A antibody (Abcam, Cambridge, MA, USA), and anti-lipoteichoic acid (LTA) antibody (Abcam) were treated to the plates for 2 h, to detect Gram-negative and Gram-positive bacterial EVs, respectively. Then, horseradish peroxidase-conjugated secondary antibody was added to the plates for 1 h and relative luminescence was measured using a chemiluminescence substrate (Roche Diagnostics GmbH, Mannheim, Germany). EVs isolated from *Escherichia coli* and *Staphylococcus aureus* as previously reported [12,24] were used as positive controls for Gram-negative and Gram-positive bacterial EVs. *E. coli* EVs and *S. aureus* EVs were also employed as negative controls for Gram-positive and Gram-negative bacterial EVs, respectively.

To examine the presence of human cell-derived EVs in the isolated indoor dust EVs, we carried out Western blotting. Briefly, indoor dust EVs (15 μg in total protein amounts) were subjected to sodium dodecyl sulphate-polyacrylamide gel electrophoresis and transferred to a polyvinylidene fluoride membrane. After blocking the membrane with 3% skim milk/TBS-T (Tween 20 0.05%) for 1 h, mouse anti-CD63, anti-CD81, anti-CD9 and anti-TSG101 (BD Biosciences, San Jose, CA, USA) were treated overnight at 4°C to detect human-derived EVs. Then horseradish peroxidase-conjugated secondary antibody (Santa Cruz Biotechnology, Santa Cruz, CA, USA) was treated for 1 h. A chemiluminescent substrate (Thermo Fisher Scientific, Waltham, MA, USA) was employed to detect the immunoreactive bands. SW480 EVs (5 μg in total protein amounts), isolated as previously described [25], were used as a positive control in Western blotting.

Melanoma lung metastasis mouse model

To assess the effects of indoor dust EVs or *P. aeruginosa* EVs on cancer lung metastasis, wild-type or TNF-α knock-out mice were anesthetized with 0.2 mL of 1.2% 2,2,2-tribromoethanol (Sigma-Aldrich). Then, a different amount of indoor dust EVs (1, 5 and 10 μg in total protein amounts) or *P. aeruginosa* EVs (10 μg in total protein amounts) in 30 μL of sterile PBS were intranasally administered to the mice. At 24 h after EV treatment, the mice were intravenously administered with B16BL6 mouse melanoma cells (5×10^4 cells), unless otherwise noted. To examine the time effect of indoor dust EV-mediated promotion of cancer lung metastasis, B16BL6 melanoma cells (5×10^4 cells) were intravenously administered to mice at day 0, and indoor dust EVs (10 μg in total protein amounts) were intranasally administered to mice at day −1 (pre-treatment), day 0 (co-treatment), as well as day +1 or +3 (post-treatment). At day 14 after tumour cell administration, the mice were sacrificed and the lungs were isolated. The lungs were bleached with 2 mL of Fekete's solution to readily visualize tumour nodules for counting colonies [26].

The lungs were also excised after whole body perfusion and fixed with 4% paraformaldehyde. After being embedded in paraffin, the lungs were then sectioned with 4 μm thickness. The lung sections were deparaffinized, rehydrated with xylene as well as escalating grades of alcohol and stained with haematoxylin and eosin. The images were acquired with a phase-contrast microscope (Carl Zeiss, Oberkochen, Germany), and colony area was determined with AxioVision Rel 4.8 Software (Carl Zeiss).

Immunohistochemistry in the lungs

To analyse tumour cell infiltration into the lungs, indoor dust EVs (10 μg in total protein amounts) were intranasally instilled to wild-type mice. At 24 h after EV instillation, B16Bl6 melanoma cells expressing enhanced green fluorescence proteins (2.5×10^5 cells) were intravenously administered to the mice. At 0 and 24 h after tumour cell administration, the mice were sacrificed and the lungs were excised after whole body perfusion. After being

fixed with 4% paraformaldehyde and embedded in paraffin, the lungs were then sectioned with 4 μm thickness. The lung sections were deparaffinized and rehydrated with xylene as well as escalating grades of ethanol. The deparaffinized lungs were soaked in target retrieval solution (DAKO, Glostrup, Denmark), and blocked with serum-free blocking solution (DAKO). The lung tissues were incubated with primary antibodies against murine CD31 (Abcam) and green fluorescence protein (Santa Cruz Biotechnology, Santa Cruz, CA, USA). After treating Alexa 555- and Alexa 488-conjugated secondary antibodies (Invitrogen, Carlsbad, CA, USA), the lung tissues were counter-stained with Hoechst (Sigma-Aldrich). The images were acquired with a confocal microscope (Carl Zeiss).

Preparation of lung lysates and NIH-3T3 conditioned media

Wild-type or TNF-α knock-out mice were intranasally administered with PBS, indoor dust EVs (10 μg in total protein amounts), or *P. aeruginosa* EVs (10 μg in total protein amounts). At 24 h after EV administration, the lungs were collected, cut into small pieces, and incubated in cold PBS (1 mL for the lungs collected from a mouse), followed by homogenization with a hand-held homogenizer (Kinetamatica GmbH, Luzern, Switzerland). The homogenized samples were subjected to centrifugation at 5000 × *g* for 5 min at 4°C, and then at 10,000 × g for 5 min at 4°C. The supernatants were filtrated with a filter with a pore size of 0.45 μm. The lung lysates were stored at −80°C until use.

To prepare NIH-3T3 conditioned media, NIH-3T3 fibroblasts were seeded at 80–90% confluency, and incubated in Dulbecco's modified Eagle's medium with 10% FBS. At 12 h after incubation, the conditioned media were harvested and subjected to centrifugation at 2,000 × *g* for 10 min at 4°C to remove remaining cells. Then, the supernatants were harvested and stored at −20°C until use.

Cell migration assay

The effects of indoor dust EVs or *P. aeruginosa* EVs on tumour cell migration were assessed using migration assay, as previously reported with some modifications [27]. An 8 μm pore-sized polycarbonate membrane (Neuro Probe, Gaithersburg, MD, USA) was treated with attachment factor protein (Gibco) for 5 min and dried for 30 min at room temperature. B16BL6 melanoma cells were labelled with 10 μM of 5-chloromethylfluorescein diacetate (CMFDA; Molecular Probes, Eugene, OR, USA) for 30 min at 37°C and then subjected to centrifugation at 150 × g for 5 min to remove remaining CMFDA. The CMFDA-labelled B16BL6 melanoma cells were resuspended in MEM with 1% FBS. A 48-well micro chemotaxis chamber (Neuro Probe) was utilized for migration assay. The CMFDA-labelled B16BL6 melanoma cells (3×10^4 cells in 30 μL of MEM with 1% FBS) were added to lower wells, and the chamber was covered with the polycarbonate membrane coated with attachment factor protein. The chamber was then assembled, inverted and incubated at 37°C for 2 h. Then, the chamber was re-inverted, the lung lysates diluted in 50 μL of MEM with 1% FBS were added to upper wells and incubated at 37°C for 3 h. The membrane was then fixed with 70% cold ethanol for 30 min. Unmigrated cells were removed, and images were acquired with a stereo microscope (Leica, Wetzlar, Germany). MEM with 1% FBS and NIH-3T3-conditioned media was utilized as negative and positive controls, respectively.

TNF-α measurement

Quantification of mouse TNF-α in the lung lysates was performed using Mouse TNF-α DuoSet ELISA kit (R&D Systems, Minneapolis, MN, USA), according to the manufacturer's instructions.

Statistical analysis

All statistical analyses were conducted using Prism 5 software (GraphPad, La Jolla, CA, USA). The values were reported as means ± standard error means (SEM) with the indicated sample sizes. Regarding *in vitro* and *in vivo* studies, the sample sizes (*n*) correspond to technical and biological replicates, respectively. *p*-values were determined by unpaired Student's *t*-test as well as one- or two-way analyses of variance (ANOVA) with Bonferroni correction for multiple comparisons. *p*-values less than 0.05 were considered as statistically significant.

Results

Characterization of indoor dust EVs

EVs were isolated from indoor dust collected from dormitory rooms. After dissolving indoor dust with PBS, insoluble matters and cell debris in indoor dust were removed with gauze and centrifugation. Indoor dust EVs were finally isolated by ultracentrifugation and buoyant density gradient ultracentrifugation. The average amount of indoor dust EVs was 22.4 ± 4.6 μg (in total protein amounts), which was equivalent to $(1.1 \pm 0.6) \times 10^{11}$ particles (in total particle counts),

from 1 g of indoor dust. Indoor dust EVs have spherical and membrane-enclosed structures, as determined by transmission electron microscopy (Figure 1(a)). Dynamic light scattering analysis showed that the average diameter of indoor dust EVs was 129.6 ± 4.5 nm (Figure 1(b)).

Then, the bacterial origin of indoor dust EVs was examined by identifying marker molecules of bacterial classes, such as lipid A, the core structure of Gram-negative bacterial lipopolysaccharides and LTA, an important component of the walls of Gram-positive bacteria. Both markers were detected in indoor dust EVs by ELISA, indicating that indoor dust contains EVs derived from Gram-negative and Gram-positive bacteria (Figure 1(c,d)). In addition, we performed Western blotting to detect human EV-enriched proteins, such as CD63, CD81, CD9 and TSG101 from indoor dust EVs. However, we could not detect the presence of any aforementioned human proteins from indoor dust EVs (Figure 1(e)). These results suggest that human cell-derived EVs are not present in the isolated indoor dust EVs.

The effects of indoor dust EVs on cancer lung metastasis

To determine the effects of indoor dust EVs on cancer lung metastasis, indoor dust EVs were intranasally administered to mice at 1 day prior to intravenous administration of B16BL6 melanoma cells. Intranasal instillation of indoor dust EVs promoted cancer lung metastasis in a dose-dependent manner (Figure 2(a,b)). About 5 and 10 μg of indoor dust EVs were sufficient to promote cancer lung metastasis, as the numbers of metastatic colonies in the lungs were significantly increased. Furthermore, histological analysis showed that metastatic colony area was increased in EV-treated group when compared with PBS-treated group (Figure 2(c,d)).

To determine the time effect of indoor dust EV-mediated promotion of cancer lung metastasis, B16BL6 melanoma cells were intravenously administered to mice at day 0, and indoor dust EVs (10 μg in total protein amounts) were intranasally instilled to mice at day −1 (pre-treatment), day 0 (co-treatment), as well as day +1 or +3 (post-treatment). Pre-treatment or co-treatment of

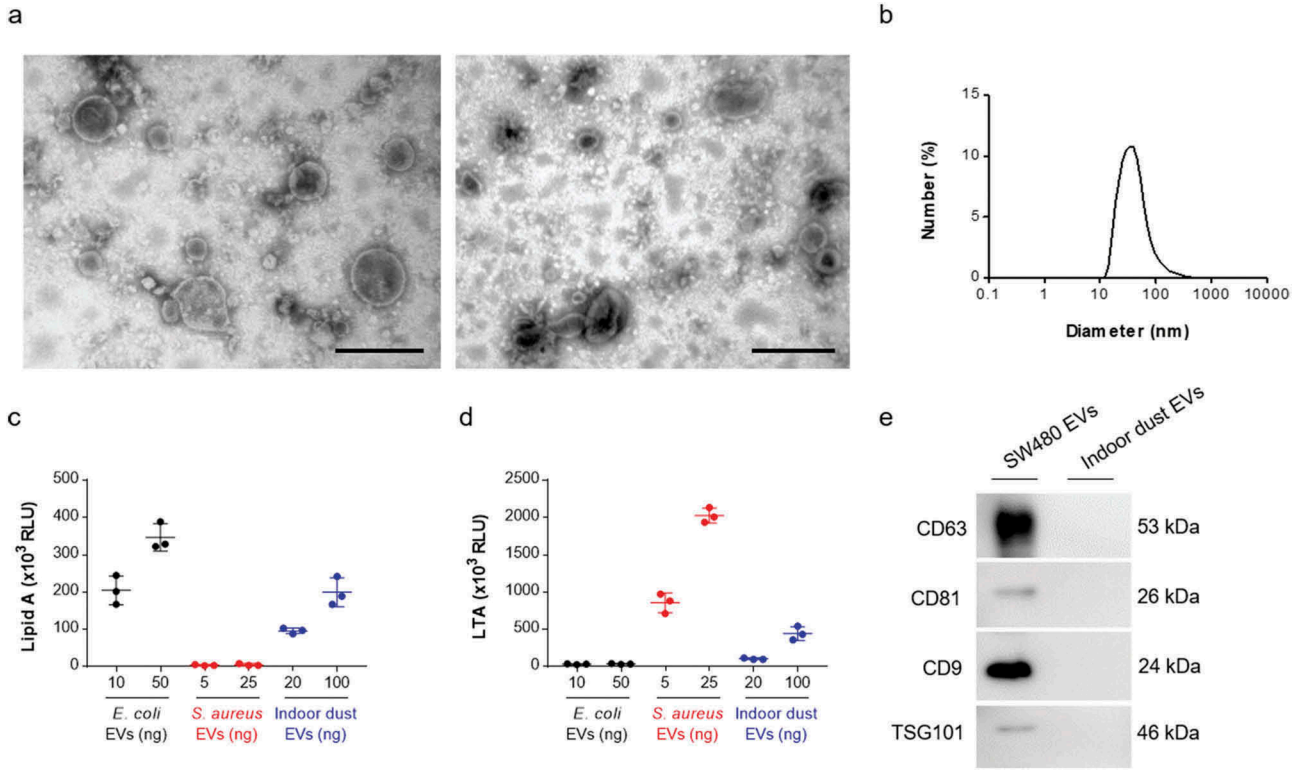

Figure 1. Characterization of indoor dust EVs. (a) Transmission electron microscopy images of indoor dust EVs. Scale bar = 200 nm. (b) The size distribution of indoor dust EVs analysed by dynamic light scattering. $n = 5$. (c, d) ELISA to detect the content of lipid A (a Gram-negative bacterial constituent) (c), and LTA (a Gram-positive bacterial constituent) (d) from indoor dust EVs (blue). *E. coli* EVs (black) and *S. aureus* EVs (red) were used as positive controls for Gram-negative and Gram-positive bacterial origins, respectively. *E. coli* EVs and *S. aureus* EVs were also employed as negative controls for Gram-positive and Gram-negative bacterial EVs, respectively. RLU, relative luminescence unit. $n = 3$. (e) Indoor dust EVs (15 μg in total protein amounts) were analysed by Western blotting, using anti-CD63, anti-CD81, anti-CD9 and anti-TSG101. SW480 EVs (5 μg in total protein amounts) were used as controls for human origins.

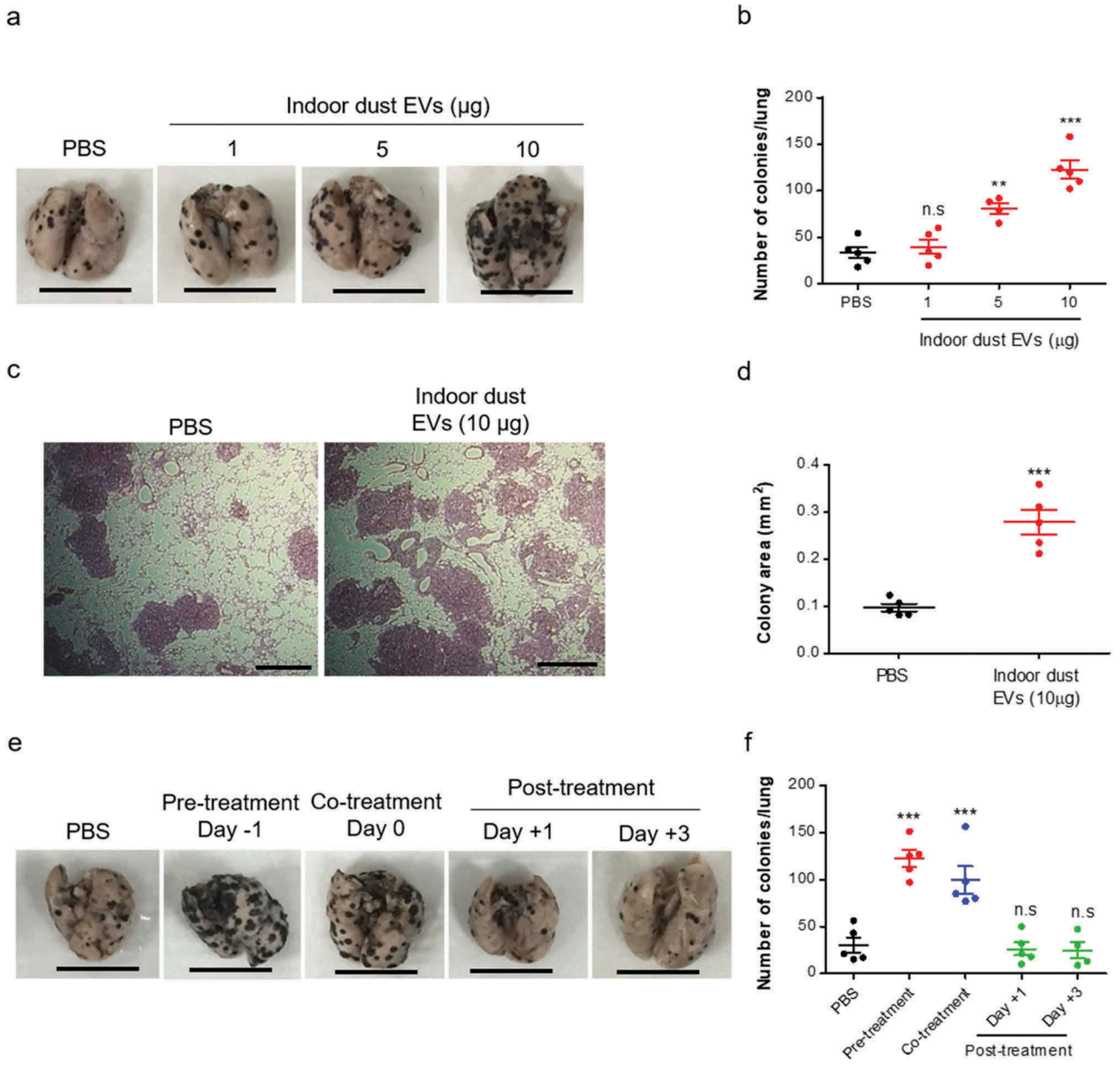

Figure 2. The effects of indoor dust EVs on cancer lung metastasis. (a, b) A dose-dependent effect of indoor dust EV-mediated promotion of melanoma lung metastasis. Mice were intranasally administered with PBS or various amounts of indoor dust EVs (1, 5 and 10 μg in total protein amounts), and at 24 h after EV administration, B16BL6 melanoma cells (5×10^4 cells) were intravenously administered to mice. At day 14 after tumour cell administration, representative images of the lungs were acquired (a), and the number of metastatic colonies in the lungs was counted (b). Scale bar = 1 cm. n = 4–5 mice per group. (c, d) Mice were intranasally administered with PBS or indoor dust EVs (10 μg in total protein amounts), and at 24 h after EV administration, B16BL6 melanoma cells (5×10^4 cells) were intravenously administered to mice. At day 14 after tumour cell administration, the lungs were collected and sectioned. The lung sections were stained with haematoxylin and eosin, and representative images of the sections were acquired with a phase-contrast microscope (c). Scale bar = 0.5 mm. Total colony area was measured from the acquired images (d). n = 5 mice per group. (e, f) The time effect of indoor dust EV-mediated promotion of cancer lung metastasis. B16BL6 melanoma cells (5×10^4 cells) were intravenously administered to mice at day 0, and indoor dust EVs (10 μg in total protein amounts) were intranasally instilled to mice at day −1 (pre-treatment), day 0 (co-treatment), as well as day +1 or +3 (post-treatment). At day 14 after tumour cell administration, representative images of the lungs were acquired (e), and the number of metastatic colonies in the lungs was counted (f). Scale bar = 1 cm. n = 4–5 mice per group. Data were represented as mean ± SEM. n.s., non-significant; $^{**}p < 0.01$ and $^{***}p < 0.001$, respectively, from comparing PBS- and indoor dust EV-treated groups, calculated by one-way ANOVA with Bonferroni correction for multiple comparisons (b, f), or unpaired Student's t-test (d).

indoor dust EVs significantly promoted cancer lung metastasis, while post-treatment of the EVs did not enhance cancer lung metastasis (Figure 2(e,f)). These results suggest that indoor dust EVs promote cancer lung metastasis in a dose-dependent manner, only when the EVs were introduced before tumour cell administration or introduced together with tumour cells.

The effects of indoor dust EVs on tumour cell migration in vivo and in vitro

To investigate the underlying mechanism responsible for promotion of cancer lung metastasis by indoor dust EVs, we examined the effects of indoor dust EVs on tumour cell infiltration into the lungs *in vivo*. At 24 h after intranasal instillation of PBS or indoor dust EVs (10 μg in total protein amounts), B16BL6 melanoma cells expressing enhanced green fluorescence proteins were intravenously introduced to the mice. At 24 h after tumour cell administration, infiltrated tumour cells (Green) were observed in the interstitial space of the lungs but not in the blood vessels (Red, stained with anti-CD31 antibody) from both PBS- and indoor dust EV-treated mice (Figure 3(a)). The number of infiltrated tumour cells was counted and indoor dust EV-treated group was approximately three times higher than PBS-treated group (Figure 3(b)).

We next investigated the effects of indoor dust EVs on tumour cell migration *in vitro*. The indoor dust EVs did not directly mediate tumour cell migration even when 1,000 ng/mL of indoor dust EVs was treated to B16BL6 cells (Supplementary Figure S1(a,b)). To determine whether indoor dust EVs induce tumour cell migration indirectly, indoor dust EVs (10 μg in total protein amounts) or PBS were intranasally introduced to mice, and the lung lysates were collected at 24 h after EV treatment. The lung lysates treated with PBS or indoor dust EVs induced tumour cell migration in a dose-dependent manner, but the lung lysates collected from indoor dust EV-treated mice mediated tumour cell migration more efficiently, approximately two times higher than ones collected from PBS-treated mice (Supplementary Figure S2(a,b)). Taken together, these results indicate that indoor dust EV-treated lung lysates could enhance tumour cell migration indirectly by undefined mechanisms, while indoor dust EVs did not directly mediate tumour cell migration *in vitro*.

The roles of TNF-α in indoor dust EV-mediated cancer lung metastasis

TNF-α has been shown to regulate tumour cell migration [28]. We found that the concentration of TNF-α was significantly increased in the lung lysates of mice at

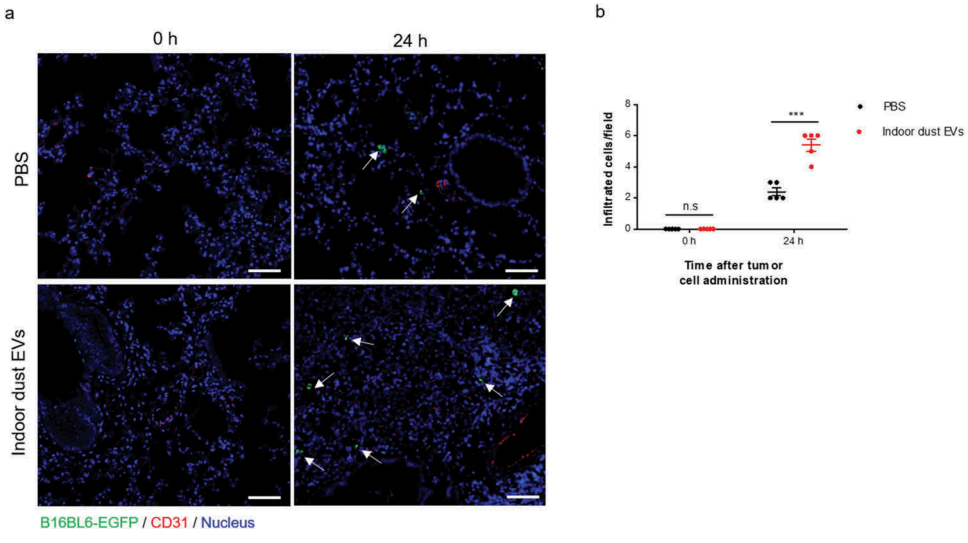

Figure 3. Indoor dust EV-mediated infiltration of tumour cells into the lungs. Mice were intranasally administered with PBS or indoor dust EVs (10 μg in total protein amounts), and at 24 h after EV administration, B16BL6 melanoma cells (2×10^5 cells) expressing enhanced green fluorescence proteins were intravenously administered to the mice. At 0 or 24 h after tumour cell administration, the lungs were collected and sectioned. The lung sections were immunostained with anti-green fluorescence protein (green, B16BL6 melanoma cells expressing enhanced green fluorescence proteins) and anti-CD31 (red, endothelial cells), then counter-stained with Hoechst (blue, nuclei). Representative images of the lung sections were acquired using a confocal microscope (a), and the number of infiltrated tumour cells was counted using the acquired images (b). White arrows indicate infiltrated tumour cells. Scale bar = 50 μm. $n = 5$ mice per group. Data were represented as mean ± SEM. n.s., non-significant; and ***$p < 0.001$, respectively, from comparing PBS- and indoor dust EV-treated groups at each time point, calculated by two-way ANOVA with Bonferroni correction for multiple comparisons.

24 h after intranasal instillation of indoor dust EVs (10 μg in total protein amounts) (Figure 4(a)). To examine the functional role of TNF-α in indoor dust EV-mediated tumour cell migration *in vitro*, indoor dust EVs (10 μg in total protein amounts) were intranasally introduced to wild-type and TNF-α knock-out mice, and the lung lysates were collected at 24 h after EV treatment. Then, tumour cells were treated with the lung lysates and subjected to migration assay. The lung lysates collected from indoor dust EV-treated wild-type mice efficiently mediated tumour cell migration, but those collected from indoor dust EV-treated TNF-α knock-out mice were much less effective in mediating tumour cell migration (Figure 4(b,c)).

To validate the functional role of TNF-α in indoor dust EV-mediated cancer lung metastasis, indoor dust EVs (10 μg in total protein amounts) were intranasally administered to mice at 1 day prior to intravenous administration of B16BL6 melanoma cells. Indoor dust EVs did not promote cancer lung metastasis in TNF-α knock-out mice, as the number of colonies metastasized to the lungs was not increased (Figure 5(a,b)). Furthermore, histological analysis confirmed that metastatic colony area was not increased in TNF-α knock-out mice treated with indoor dust EVs (Figure 5(c,d)). Taken together, these results suggest that TNF-α plays a critical role in promotion of cancer lung metastasis mediated by indoor dust EVs.

The effects of *P. aeruginosa* EVs on cancer lung metastasis and the roles of TNF-α in *P. aeruginosa* EV-mediated cancer lung metastasis

To identify bacteria which produced indoor dust EVs, we performed reverse transcriptase-polymerase chain reaction and 16 S rRNA sequencing using indoor dust EVs as templates. The major species belonged to *Pseudomonas* genus, with percentage identity more than 97% (Supplementary Table S1). As a representative *Pseudomonas* species, we cultured *P. aeruginosa* and purified EVs from the bacterial culture. *P. aeruginosa* EVs have spherical and membrane-enclosed structures, as determined by transmission electron microscopy (Figure 6(a)). Dynamic light scattering analysis showed that the average diameter of *P. aeruginosa* EVs was 81.9 ± 2.5 nm (Figure 6(b)).

To determine the effects of *P. aeruginosa* EVs on cancer lung metastasis, *P. aeruginosa* EVs or indoor dust EVs were intranasally administered to mice at 1 day prior to intravenous administration of B16BL6 melanoma cells. Intranasal instillation of *P. aeruginosa* EVs promoted cancer lung metastasis, and the effects were comparable with indoor dust EVs (Figure 6(c,d)).

Furthermore, as in the case of indoor dust EVs, we found that the concentration of TNF-α was significantly increased in the lung lysates of mice at 24 h after intranasal instillation of *P. aeruginosa* EVs (10 μg in total protein

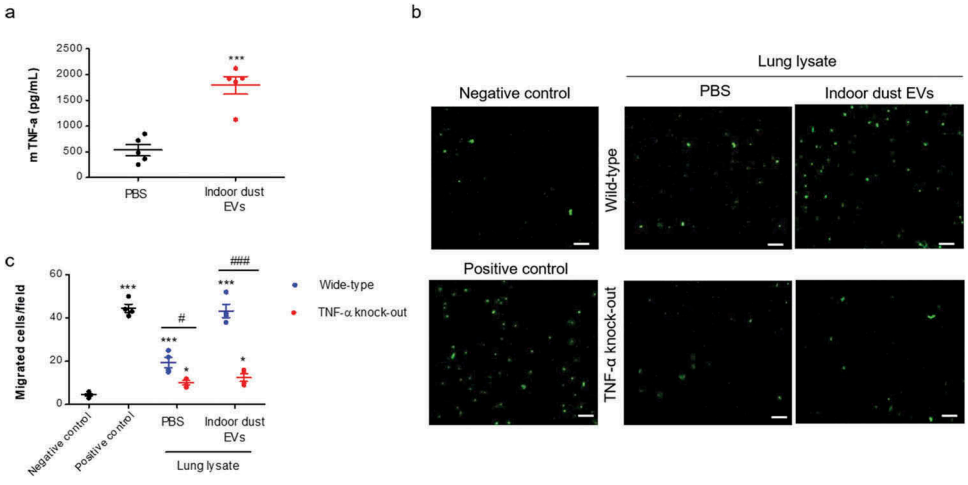

Figure 4. The role of TNF-α in indoor dust EV-mediated tumour cell migration *in vitro*. Wild-type and TNF-α knock-out mice were intranasally administered with PBS or indoor dust EVs (10 μg in total protein amounts). At 24 h after EV administration, the lungs were collected and the lung lysates were prepared for further experiments. (a) The concentration of TNF-α in the lung lysates of wild-type mice. $n = 5$ mice per group. (b, c) The lung lysates of wild-type and TNF-α knock-out mice were used for migration assay. CMFDA-labelled B16BL6 melanoma cells were treated with the lung lysates (dilution fold: 1:5) for 3 h to observe tumour cell migration. Representative images of migrated tumour cells were acquired using a stereo microscope (b), and the number of migrated tumour cells was counted using the images (c). MEM with 1% FBS and NIH3T3 conditioned media were used as negative and positive controls. Scale bar = 50 μm. $n = 4$ mice per group. Data were represented as mean ± SEM. $^{*}p < 0.05$ and $^{***}p < 0.001$, respectively, from comparing PBS or the negative control with other groups. $^{\#}p < 0.05$ and $^{\#\#\#}p < 0.001$ from comparing the groups treated with the lung lysates from wild-type and TNF-α knock-out mice. *p*-values were calculated using unpaired Student's *t*-test (a) or two-way ANOVA with Bonferroni correction for multiple comparisons (c).

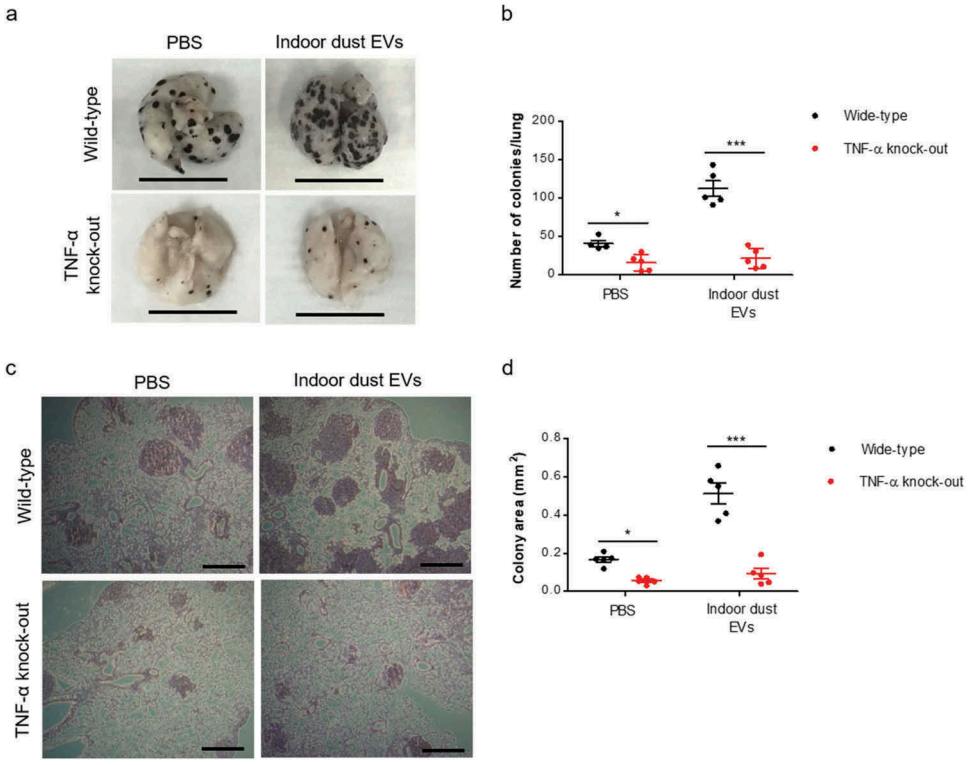

Figure 5. The roles of TNF-α in indoor dust EV-mediated cancer lung metastasis *in vivo*. Wild-type and TNF-α knock-out mice were intranasally administered with PBS or indoor dust EVs (10 μg in total protein amounts), and at 24 h after EV administration, B16BL6 melanoma cells (5×10^4 cells) were intravenously administered to mice. At day 14 after tumour cell administration, the lungs were collected. (a, b) Representative images of the lungs were acquired (a), and the number of metastatic colonies in the lungs was counted (b). Scale bar = 1 cm. (c, d) The lung sections were stained with haematoxylin and eosin, and representative images of the sections were acquired with a phase-contrast microscope (c). Scale bar = 0.5 mm. Total colony area was measured from the acquired images (d). $n = 5$ mice per group. $^*p < 0.05$ and $^{***}p < 0.001$ from comparing the groups treated with PBS and indoor dust EVs from wild-type and TNF-α knock-out mice. *p*-values were calculated using two-way ANOVA with Bonferroni correction for multiple comparisons.

amounts) (Figure 7(a)). To examine the functional roles of TNF-α in *P. aeruginosa* EV-mediated tumour cell migration *in vitro*, *P. aeruginosa* EVs (10 μg in total protein amounts) were intranasally introduced to wild-type and TNF-α knock-out mice, and the lung lysates were collected at 24 h after EV treatment. Then, tumour cells were treated with the lung lysates and subjected to migration assay. The lung lysates collected from *P. aeruginosa* EV-treated wild-type mice efficiently mediated tumour cell migration, but those collected from *P. aeruginosa* EV-treated TNF-α knock-out mice were much less effective in mediating tumour cell migration (Figure 7(b)).

Finally, to validate the functional role of TNF-α in *P. aeruginosa* EV-mediated cancer lung metastasis, *P. aeruginosa* EVs (10 μg in total protein amounts) were intranasally administered to mice at 1 day prior to intravenous administration of B16BL6 melanoma cells. *P. aeruginosa* EVs did not promote cancer lung metastasis in TNF-α knock-out mice, as the number of colonies metastasized to the lungs was not increased (Figure 7(c,d)). Taken together, these results suggest that *P. aeruginosa* EVs, at least partly, contributed to the effects of indoor dust EVs in promoting cancer lung metastasis and TNF-α plays a critical role in promotion of cancer lung metastasis mediated by *P. aeruginosa* EVs.

Discussion

While indoor dust EVs have been reported to mediate pulmonary inflammation, and to be associated with various lung diseases [5,14], their roles in tumour metastasis have not been examined yet. In this study, we provided evidences that indoor dust EVs could promote cancer lung metastasis in the mouse metastatic melanoma model in a dose-dependent manner, only when the EVs were introduced before or together with tumour cell administration. Indoor dust EVs enhanced tumour cell infiltration into the lungs *in vivo*, although indoor dust EVs did not directly mediate tumour cell migration *in vitro*. TNF-α played

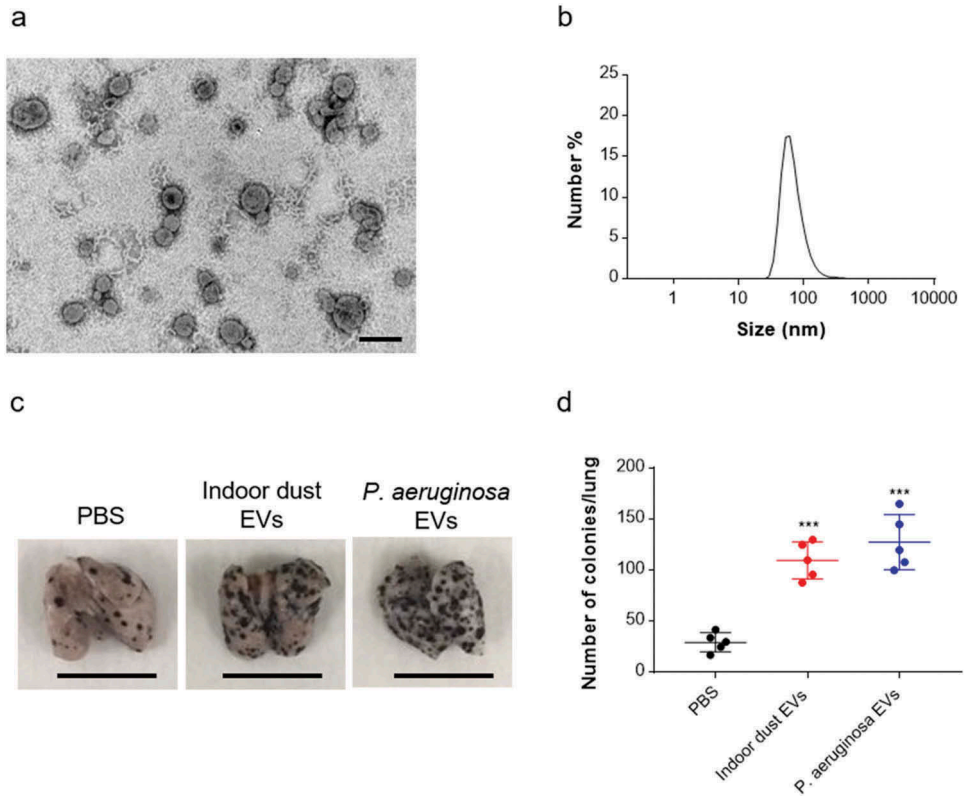

Figure 6. The effects of *P. aeruginosa* EVs on cancer lung metastasis. (a, b) Characterization of *P. aeruginosa* EVs. (a) Transmission electron microscopy images of *P. aeruginosa* EVs. Scale bar = 200 nm. (b) The size distribution of *P. aeruginosa* EVs analysed by dynamic light scattering. $n = 5$. (c, d) Comparison of the effects of indoor dust EVs and *P. aeruginosa* EVs on cancer lung metastasis. Mice were intranasally administered with PBS, indoor dust EVs (10 μg in total protein amounts), or *P. aeruginosa* EVs (10 μg in total protein amounts), and at 24 h after EV administration, B16BL6 melanoma cells (5×10^4 cells) were intravenously administered to mice. At day 14 after tumour cell administration, representative images of the lungs were acquired (c), and the number of metastatic colonies in the lungs was counted (d). Scale bar = 1 cm. $n = 5$ mice per group. Data were represented as mean SEM. ***$p < 0.001$ from comparing the EV-treated groups with PBS-treated group. *p*-values were determined using one-way ANOVA with Bonferroni correction for multiple comparisons.

important roles in indoor dust EV-mediated tumour cell migration *in vitro* and in cancer lung metastasis *in vivo*. The clinical implication of this study can be confirmed by a reliable method to quantify the concentration of indoor dust EVs in a defined volume of indoor air, and to measure the volume of indoor air that a person inhales in a defined period of time. However, the quantification of EVs is limited by current EV detection techniques [29]. The plausible doses in humans and the effects of chronic exposure should be carefully investigated in further studies.

Our data showed that indoor dust EVs harboured both Gram-negative and Gram-positive bacterial EVs, as identified by specific markers, lipid A and LTA. Bacteria are common microbes present in indoor dust [6,30], and indoor dust EVs, especially Gram-negative bacterial EVs, have been reported to induce pulmonary inflammation [5]. In addition, Gram-negative bacteria have been demonstrated to facilitate tumour metastasis [31,32]. Indeed, by 16 S rRNA sequencing using indoor dust EVs, we identified that *Pseudomonas* genus is the major bacterial genus that produce indoor dust EVs. We found that *P. aeruginosa* EVs and indoor dust EVs showed comparable effects in promoting tumour cell migration *in vitro* and cancer lung metastasis *in vivo*. In addition, TNF-α plays a critical role in promotion of *P. aeruginosa* EV-mediated cancer lung metastasis as observed in indoor dust EVs. Thus, *Pseudomonas* EVs, at least partly, contributed to the effects of indoor dust EVs in promoting cancer lung metastasis. However, additional studies will be required to determine the contributions of Gram-negative and Gram-positive bacterial EVs in indoor dust EV-mediated promotion of cancer lung metastasis. The contributions of bacterial species or genera would also be valuable to develop preventive strategies against indoor dust EV-mediated promotion of cancer lung metastasis.

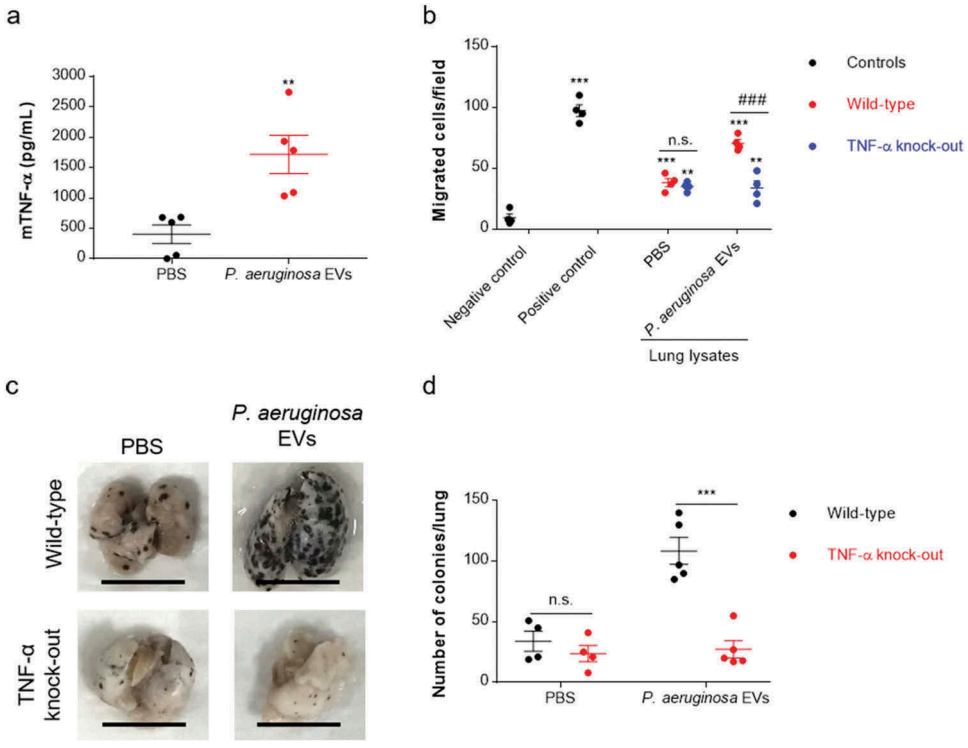

Figure 7. The roles of TNF-α in *P. aeruginosa* EV-mediated tumour cell migration *in vitro* and cancer lung metastasis *in vivo*. (a, b) The role of TNF-α in *P. aeruginosa* EV-mediated tumour cell migration *in vitro*. Wild-type and TNF-α knock-out mice were intranasally administered with PBS or *P. aeruginosa* EVs (10 μg in total protein amounts). At 24 h after EV administration, the lungs were collected and the lung lysates were prepared for further experiments. (a) The concentration of TNF-α in the lung lysates of wild-type mice. $n = 5$ mice per group. (b) The lung lysates of wild-type and TNF-α knock-out mice were used for migration assay. CMFDA-labelled B16BL6 melanoma cells were treated with the lung lysates (dilution fold: 1:5) for 3 h to observe tumour cell migration. The number of migrated tumour cells was counted. MEM with 1% FBS and NIH3T3 conditioned media were used as negative and positive controls. Scale bar = 50 μm. $n = 4$ mice per group. Data were represented as mean ± SEM. $^{**}p < 0.01$ and $^{***}p < 0.001$, respectively, from comparing PBS or the negative control with other groups. n.s., non-significant; and $^{\#\#\#}p < 0.001$ from comparing the groups treated with the lung lysates from wild-type and TNF-α knock-out mice. P-values were calculated using unpaired Student's *t*-test (a) or two-way ANOVA with Bonferroni correction for multiple comparisons (b). (c, d) The role of TNF-α in *P. aeruginosa* EV-mediated cancer lung metastasis *in vivo*. Wild-type and TNF-α knock-out mice were intranasally administered with PBS or *P. aeruginosa* EVs (10 μg in total protein amounts), and at 24 h after EV administration, B16BL6 melanoma cells (5×10^4 cells) were intravenously administered to mice. At day 14 after tumour cell administration, the lungs were collected. Representative images of the lungs were acquired (c), and the number of metastatic colonies in the lungs was counted (d). Scale bar = 1 cm. $n = 5$ mice per group. Data were represented as mean ± SEM. n.s., non-significant; and $^{***}p < 0.001$ from comparing the groups treated with PBS and *P. aeruginosa* EVs from wild-type and TNF-α knock-out mice. *p*-values were calculated using two-way ANOVA with Bonferroni correction for multiple comparisons.

We employed intravenous administration of tumour cells as a metastasis mouse model to investigate the effects of tissue microenvironment to tumour metastasis [33]. This model can be utilized to assess two important steps of tumour metastasis: extravasation and tumour cell growth in the metastasized sites [34]. Using this model, indoor dust EVs were administered before (pre-treatment) or after (post-treatment) tumour cell administration, as well as introduced together with tumour cells (co-treatment). Pre- and co-treatment could affect both extravasation and tumour cell growth in the metastasized sites, whereas post-treatment could mainly affect tumour cell growth in the metastasized site. We found that pre-treatment or co-treatment of indoor dust EVs significantly promoted cancer lung metastasis, whereas post-treatment of the EVs did not enhance cancer lung metastasis. In addition, we showed that indoor dust EVs enhanced tumour cell migration indirectly. As tumour cell migration is critical for the extravasation of circulating tumour cells [35,36], it seems that indoor dust EVs might be involved in the extravasation step.

However, we could not exclude the other possibility that indoor dust EVs could exert certain effects on tumour cell growth at the metastasized sites. Angiogenesis is an important process to support tumour cell growth at the metastasized sites [37]. Therefore, assessing the effects of indoor dust EVs on lung neovascularization *in vivo* or indoor dust EV-treated lung lysates on tube formation *in vitro* will

provide key evidences to understand how indoor dust EVs are involved in angiogenesis, which is subsequently affect tumour cell growth at the metastasized sites. Furthermore, we found an increase of plasma leakage in the lungs at 24 h after intranasal instillation of indoor dust EVs (Supplementary Figure S3), suggesting that indoor dust EVs could induce vascular leakiness in the lungs. Further studies are required to determine whether indoor dust EV-induced increase of vascular leakiness in the lungs promotes tumour cell migration and metastasis to the lungs.

TNF-α has been reported to be associated with promoting tumour metastasis, as it can regulate different pro-metastatic processes, including triggering tumour cell proliferation, promoting angiogenesis, recruiting other metastasis-supporting cells and increasing tumour cell migration [28,38,39]. Indeed, TNF-α significantly enhanced cancer lung metastasis in an experimental fibrosarcoma metastasis model [40]. In addition, lung and liver metastases were markedly reduced in TNF-α and TNF-α receptor knock-out mice, respectively [41,42]. Therefore, targeting TNF-α may be a promising strategy to reduce tumour metastasis. A current study showed that etanercept (a TNF-α inhibitor) and infliximab (an antibody neutralizing TNF-α) may possibly attenuate tumour metastasis in experimental mouse models [43].

In conclusion, we present here for the first time that indoor dust EVs have the capacity to promote cancer lung metastasis when intranasally instilled before or together with tumour cell administration. These promoting effects seem to be mediated through increasing tumour cell migration and attenuated in TNF-α knock-out mice. Our study will contribute to understanding the mechanisms underlying the association of indoor pollutants and public health.

Author contributions

N. T. H. D., J. L. and Y. S. G. conceived and designed the research. N. T. H. D., J. L., JaeminL, S. S. K., G. G., S. B., Y. I. J. and Y. J. Y. performed the experiments. N. T. H. D., J. L., T. Y. R. and Y. S. G. analyzed and interpreted the data. N. T. H. D., J. L., T. Y. R. and Y. S. G. wrote the manuscript.

Disclosure statement

The authors report no conflicts of interest.

Funding

This work was supported by the National Research Foundation of Korea (NRF) grant funded by the Korea government (MIST) (No. 2018R1A2A1A05079510).

References

[1] Seguel JM, Merrill R, Seguel D, et al. Indoor air quality. Am J Lifestyle Med. 2017;11:284–295.
[2] Klepeis NE, Nelson WC, Ott WR, et al. The national human activity pattern survey (NHAPS): a resource for assessing exposure to environmental pollutants. J Expo Anal Environ Epidemiol. 2001;11: 231–252.
[3] Cincinelli A, Martellini T. Indoor air quality and health. Int J Environ Res Public Health. 2017;14:1286.
[4] Weikl F, Tischer C, Probst AJ, et al. Fungal and bacterial communities in indoor dust follow different environmental determinants. PLoS One. 2016;11: e0154131.
[5] Kim YS, Choi EJ, Lee WH, *et al*. Extracellular vesicles, especially derived from Gram-negative bacteria, in indoor dust induce neutrophilic pulmonary inflammation associated with both Th1 and Th17 cell responses. Clin Exp Allergy. 2013;43:443–454.
[6] Barberan A, Dunn RR, Reich BJ, *et al*. The ecology of microscopic life in household dust. Proc Biol Sci. 2015;282(1814):20151139.
[7] Yoon YJ, Kim OY, Gho YS. Extracellular vesicles as emerging intercellular communicasomes. BMB Rep. 2014;47:531–539.
[8] Zaborowski MP, Balaj L, Breakefield XO, et al. Extracellular vesicles: composition, biological relevance, and methods of study. Bioscience. 2015;65:783–797.
[9] Deatherage BL, Cookson BT. Membrane vesicle release in bacteria, eukaryotes, and archaea: a conserved yet underappreciated aspect of microbial life. Infect Immun. 2012;80:1948–1957.
[10] Tetta C, Ghigo E, Silengo L, et al. Extracellular vesicles as an emerging mechanism of cell-to-cell communication. Endocrine. 2013;44:11–19.
[11] van Niel G, D'Angelo G, Raposo G. Shedding light on the cell biology of extracellular vesicles. Nat Rev Mol Cell Biol. 2018;19:213–228.
[12] Lee EY, Choi DY, Kim DK, *et al*. Gram-positive bacteria produce membrane vesicles: proteomics-based characterization of *Staphylococcus aureus*-derived membrane vesicles. Proteomics. 2009;9:5425–5436.
[13] Gho YS, Lee C. Emergent properties of extracellular vesicles: a holistic approach to decode the complexity of intercellular communication networks. Mol Biosyst. 2017;13:1291–1296.
[14] Kim YS, Choi JP, Kim MH, *et al*. IgG sensitization to extracellular vesicles in indoor dust is closely associated with the prevalence of non-eosinophilic asthma, COPD, and lung cancer. Allergy Asthma Immunol Res. 2016;8:198–205.
[15] Seyfried TN, Huysentruyt LC. On the origin of cancer metastasis. Crit Rev Oncog. 2013;18:43–73.
[16] Welch DR, Hurst DR. Defining the hallmarks of metastasis. Cancer Res. 2019;79:3011–3027.
[17] Fidler IJ. The pathogenesis of cancer metastasis: the 'seed and soil' hypothesis revisited. Nat Rev Cancer. 2003;3:453–458.
[18] Viegi G, Simoni M, Scognamiglio A, et al. Indoor air pollution and airway disease. Int J Tuberc Lung Dis. 2004;8:1401–1415.

[19] Hulin M, Simoni M, Viegi G, et al. Respiratory health and indoor air pollutants based on quantitative exposure assessments. Eur Respir J. 2012;40:1033–1045.
[20] Budczies J, von Winterfeld M, Klauschen F, *et al*. The landscape of metastatic progression patterns across major human cancers. Oncotarget. 2015;6:570–583.
[21] Van Deun J, Mestdagh P, Agostinis P, *et al*. EV-TRACK: transparent reporting and centralizing knowledge in extracellular vesicle research. Nat Methods. 2017;14:228–232.
[22] Choi DS, Kim DK, Choi SJ, et al. Proteomic analysis of outer membrane vesicles derived from *Pseudomonas aeruginosa*. Proteomics. 2011;11:3424–3429.
[23] Go G, Lee J, Choi DS, et al. Extracellular vesicle-mimetic ghost nanovesicles for delivering anti-inflammatory drugs to mitigate Gram-negative bacterial outer membrane vesicle-induced systemic inflammatory response syndrome. Adv Healthc Mater. 2019;8:e1801082.
[24] Lee J, Yoon YJ, Kim JH, *et al*. Outer membrane vesicles derived from *Escherichia coli* regulate neutrophil migration by induction of endothelial IL-8. Front Microbiol. 2018;9:2268.
[25] Choi DS, Choi DY, Hong BS, et al. Quantitative proteomics of extracellular vesicles derived from human primary and metastatic colorectal cancer cells. J Extracell Vesicles. 2012;1:18704.
[26] Overwijk WW, Restifo NP. B16 as a mouse model for human melanoma. Curr Protoc Immunol. 2001. Chapter 20, Unit 20.1:1–29.
[27] Kim CW, Lee HM, Lee TH, et al. Extracellular membrane vesicles from tumor cells promote angiogenesis via sphingomyelin. Cancer Res. 2002;62:6312–6317.
[28] Wu Y, Zhou BP. TNF-alpha/NF-kappaB/Snail pathway in cancer cell migration and invasion. Br J Cancer. 2010;102:639–644.
[29] Thery C, Witwer KW, Aikawa E, *et al*. Minimal information for studies of extracellular vesicles 2018 (MISEV2018): a position statement of the international society for extracellular vesicles and update of the MISEV2014 guidelines. J Extracell Vesicles. 2018;7:1535750.
[30] Dunn RR, Fierer N, Henley JB, et al. Home life: factors structuring the bacterial diversity found within and between homes. PLoS One. 2013;8:e64133.
[31] Yan L, Cai Q, Xu Y. The ubiquitin-CXCR4 axis plays an important role in acute lung infection-enhanced lung tumor metastasis. Clin Cancer Res. 2013;19:4706–4716.
[32] Ye M, Gu X, Han Y, et al. Gram-negative bacteria facilitate tumor outgrowth and metastasis by promoting lipid synthesis in lung cancer patients. J Thorac Dis. 2016;8:1943–1955.
[33] Khanna C, Hunter K. Modeling metastasis *in vivo*. Carcinogenesis. 2005;26:513–523.
[34] Gomez-Cuadrado L, Tracey N, Ma R, et al. Mouse models of metastasis: progress and prospects. Dis Model Mech. 2017;10:1061–1074.
[35] Sahai E. Illuminating the metastatic process. Nat Rev Cancer. 2007;7:737–749.
[36] Strilic B, Offermanns S. Intravascular survival and extravasation of tumor cells. Cancer Cell. 2017;32:282–293.
[37] Folkman J. Role of angiogenesis in tumor growth and metastasis. Semin Oncol. 2002;29:15–18.
[38] Ham B, Fernandez MC, D'Costa Z, et al. The diverse roles of the TNF axis in cancer progression and metastasis. Trends Cancer Res. 2016;11:1–27.
[39] Psaila B, Lyden D. The metastatic niche: adapting the foreign soil. Nat Rev Cancer. 2009;9:285–293.
[40] Orosz P, Echtenacher B, Falk W, et al. Enhancement of experimental metastasis by tumor necrosis factor. J Exp Med. 1993;177:1391–1398.
[41] Kitakata H, Nemoto-Sasaki Y, Takahashi Y, et al. Essential roles of tumor necrosis factor receptor p55 in liver metastasis of intrasplenic administration of colon 26 cells. Cancer Res. 2002;62:6682–6687.
[42] Kim S, Takahashi H, Lin WW, et al. Carcinoma-produced factors activate myeloid cells through TLR2 to stimulate metastasis. Nature. 2009;457:102–106.
[43] Egberts JH, Cloosters V, Noack A, *et al*. Anti-tumor necrosis factor therapy inhibits pancreatic tumor growth and metastasis. Cancer Res. 2008;68:1443–1450.